# Information–Theoretic Oracle Based on Kernel Smoothness for Hierarchical Radiosity

Miquel Feixas[†], Jaume Rigau[‡], Philippe Bekaert[§], and Mateu Sbert[¶]

[†‡¶] Institut d'Informàtica i Aplicacions, Universitat de Girona, Spain
[§] Max-Planck-Institut fuer Informatik, Germany

**Abstract**

*One of the main problems in the radiosity method is how to discretise the surfaces of a scene into mesh elements that allow us to accurately represent illumination. In this paper we present a robust information-theoretic refinement criterion (oracle) based on kernel smoothness for hierarchical radiosity. This oracle improves on previous ones in that at equal cost it gives a better discretisation, approaching the optimal one from an information theory point of view, and also needs less visibility computations for a similar image quality.*

Categories and Subject Descriptors (according to ACM CCS): I.3.7 [Three-Dimensional Graphics and Realism]: Radiosity.

## 1. Introduction

In the radiosity method, scene meshing has to accurately represent illumination variations. At the same time, it has to avoid unnecessary subdivisions that would increase the computation time. A correct strategy should try to balance accuracy and computational cost.

Hierarchical techniques [10, 2] aim at this target. They introduce an oracle upon which a decision to subdivide is made. The oracle should be intelligent enough to ask for more subdivision where more precision is needed. On the other hand, its cost should not make the method prohibitive.

The cheapest and most used oracle has been the power-based oracle [10]. However, it leads to unnecessary subdivisions in smoothly illuminated unoccluded regions receiving a lot of power. As an alternative, oracles based on the smoothness of the geometrical kernel (point-to-point form factors) and the received radiosity have been proposed [16, 8, 13, 14, 12, 3, 17, 11]. However, oracles based on kernel smoothness have also the problem of unnecessary subdivisions where the kernel is unbounded, and the ones based on received radiosity rely on a costly accurate computation of form factors. All in all, the additional cost invested in both smoothness-based oracles, mainly through visibility computations, may not be balanced by the obtained improvements.

In this paper we present a kernel smoothness based oracle which has a robust behaviour, i.e., we can decrease the needed additional visibility tests to just a few and still get an accurate decision. This oracle comes from the previous results obtained by the authors on information theory applications to radiosity, and differs from a previous oracle proposal [6], based on the estimated increase of discrete radiosity mutual information, in the sense that here we use the knowledge of how far we are from the perfect discretisation from an information-theoretic perspective. Specifically, the difference between continuous and discrete element-to-element mutual information will make the basis for our oracle.

The paper is organised as follows: First (section 2), we review different refinement oracles used in the hierarchical radiosity setting, and also information theory tools for scene discretisation. In section 3, we introduce the continuous radiosity mutual information and we propose a new oracle based on the difference between continuous and discrete element-to-element mutual information. In section 4, some experiments show the better discretisation and robustness of our method in comparison with a classic smoothness-based

† miquel.feixas@udg.es
‡ jaume.rigau@udg.es
§ Philippe.Bekaert@mpi-sb.mpg.de
¶ mateu.sbert@udg.es

oracle. And finally, in section 5, we present our conclusions and future work.

## 2. Previous Work

In this section we give an overview of different refinement oracles used in the hierarchical radiosity setting [1], and also some information theory tools for scene discretisation introduced in [5, 6].

### 2.1. Refinement Criteria

The application of a good refinement criterion and strategy is fundamental for the efficiency of the hierarchical refinement algorithm. Next we review some criteria proposed in the past.

#### Refinement based on transported power

Hierarchical refinement radiosity was initially presented for constant radiosity approximations by Hanrahan et al. [10]. A cheap form factor estimate $\tilde{F}_{ij}$ ignoring visibility was used to measure the accuracy of a candidate interaction from an element $j$ to an element $i$. If $\max(\tilde{F}_{ij}, \tilde{F}_{ji})$ exceeds a given threshold $\varepsilon$, the larger of the two elements $i$ and $j$ is subdivided using regular quadtree subdivision. In the other case, the candidate link is considered admissible.

Hanrahan et al. [10] also observed that the number of form factors can be reduced considerably without affecting image quality by weighting the link error estimates $\tilde{F}_{ij}$ with the source element radiosity $B_j$ and receiver element area $A_i$. Weighting with receiver reflectance $\rho_i$ also further reduces the number of links without deteriorating image quality. The power-based oracle used in our comparisons is given by

$$\rho_i A_i \tilde{F}_{ij} B_j < \varepsilon \qquad (1)$$

Other strategies [18, 7] can be used to reduce the number of form factors by taking visibility information about candidate interactions into account. Let us observe that form-factor and power-based refinement criteria use no information about the variation of the received radiosity across the receiver element. This results for instance in sub-optimal shadow boundaries and too fine refinement in smooth areas. The main advantage of this criterion is its very low computational cost while yielding a fair image quality.

#### Refinement based on kernel smoothness

In order to improve on power-based refinement, the variation of the radiosity kernel $G(x,y)$ between a pair of elements is taken into account. $G(x,y)$ is equal to $F(x,y)vis(x,y)$, where $F(x,y)$ is the point-to-point form factor without occlusion and $vis(x,y)$ takes the value 1 if $x$ and $y$ are mutually visible and 0 otherwise.

In [16], the refinement criterion is given by $\rho_i(G_{ij}^{max} - G_{ij}^{min})A_jB_j < \varepsilon$ where $G_{ij}^{max} = max_{x\in\mathcal{S}_i, y\in\mathcal{S}_j} G(x,y)$ and $G_{ij}^{min} = min_{x\in\mathcal{S}_i, y\in\mathcal{S}_j} G(x,y)$ are the maximum and minimum radiosity kernel values and are estimated by taking the maximum and minimum value computed between pairs of random points on both elements, $\mathcal{S}_i$ and $\mathcal{S}_j$ are the surfaces of the elements, $\varepsilon$ is a predefined threshold, $A_j$, $B_j$, $\rho_i$ are respectively the source area, source radiosity, and receiver reflectivity.

A similar approach was used in [8] in order to drive hierarchical refinement with higher-order approximations. When applied to constant approximations, the refinement criterion is given by

$$\rho_i max(G_{ij}^{max} - G_{ij}^{av}, G_{ij}^{av} - G_{ij}^{min})A_jB_j < \varepsilon \qquad (2)$$

where $G_{ij}^{av}$ is the average radiosity kernel value, $G_{ij}^{av} = F_{ij}/A_j$, and $F_{ij}$ is the form factor between patches $i$ and $j$. Kernel variation is a sufficient condition for received radiosity variation, but not a necessary condition [1].

#### Refinement based on smoothness of received radiosity

Because bounding kernel variation is not a necessary condition for bounding received radiosity variation, we can expect that hierarchical refinement based on kernel smoothness will yield hierarchical meshes with more elements and links than required. Optimal refinement can be expected by directly estimating how well the radiosity $B_j(x)$ received at $x \in S_i$ from $S_j$ is approximated by a linear combination of the basis functions on $S_i$, i.e. by estimating the discretisation error directly.

This approach was first proposed by Lischinski et al. [13] for constant approximations and Pattanaik and Bouatouch [14] proposed a similar strategy for linear basis functions. Other approaches are given in [12, 3, 17, 11]. The computation cost of kernel and radiosity smoothness-based oracles was not yet found to compensate for the gain in mesh quality [1].

### 2.2. Information Theory Tools

In [5], discrete ($I_v^d$) and continuous ($I_v^c$) visibility mutual information have been introduced as scene complexity measures, and also discrete mutual information was generalized to the radiosity setting ($I_r^d$). These complexity measures represent the visibility information transfer in a scene and express the difficulty of discretising it: the higher the continuous mutual information, the more difficult it is to obtain an accurate discretisation and probably more refinements are necessary to achieve a predefined precision.

In [5, 6], the following results and proposals concerning visibility and radiosity were presented:

- Continuous mutual information $I^c$ is the least upper bound to discrete mutual information $I^d$.
- $I^c$, independent of any discretisation, expresses with maximum accuracy the information transfer or dependence in a scene.
- By refining the patches, $I^d$ must increase (or remain the same).

- Among different discretisations of a scene the most accurate one is the one with the highest discrete mutual information, i.e. with minimum loss of information transfer.
- A global discretisation error can be given by

$$\Delta = \frac{I^c - I^d}{I^c}$$

Discrete scene radiosity mutual information, introduced in [5], is given by

$$I_r^d = \sum_{i=1}^{n_p} \sum_{j=1}^{n_p} \frac{\mathcal{A}_i \mathcal{F}_{ij}}{\mathcal{A}_T} \log\Big(\frac{\mathcal{F}_{ij}\mathcal{A}_T}{\mathcal{A}_j}\Big) \tag{3}$$

where logarithms are in base 2, $n_p$ is the number of patches, $\mathcal{A}_i = A_i \frac{(B_i - E_i)}{\rho_i} B_i$, $\mathcal{A}_T = \sum_i \mathcal{A}_i$, $\mathcal{F}_{ij} = \frac{\rho_i F_{ij} B_j}{B_i - E_i}$, $F_{ij}$ is the form factor between patches $i$ and $j$, and $E_i$, $B_i$, $\rho_i$, and $A_i$ are respectively the emission, radiosity, reflectivity, and area of patch $i$.

From (3), the term

$$I_{r_{ij}}^d = \frac{\mathcal{A}_i \mathcal{F}_{ij}}{\mathcal{A}_T} \log\Big(\frac{\mathcal{F}_{ij}\mathcal{A}_T}{\mathcal{A}_j}\Big) \tag{4}$$

can be considered as an element of a mutual information matrix, and it is easy to see that $I_{r_{ij}}^d = I_{r_{ji}}^d$. Each element represents the radiosity information transfer between patches $i$ and $j$. Also, we can consider that

$$I_{r_i}^d = \sum_{j=1}^{n_p} \frac{\mathcal{A}_i \mathcal{F}_{ij}}{\mathcal{A}_T} \log\Big(\frac{\mathcal{F}_{ij}\mathcal{A}_T}{\mathcal{A}_j}\Big) \tag{5}$$

expresses the information transfer from patch $i$. Thus,

$$I_r^d = \sum_{i=1}^{n_p} I_{r_i}^d = \sum_{i=1}^{n_p} \sum_{j=1}^{n_p} I_{r_{ij}}^d \tag{6}$$

If we analyze the terms $I_{r_{ij}}^d$ we observe that negative values appear when $\mathcal{F}_{ij} < \mathcal{A}_j$. This situation reflects a very low interaction between the two patches involved. On the other hand, using the concavity property of the logarithm function[4]

$$\sum_{k=1}^{n} a_k \log\Big(\frac{a_k}{b_k}\Big) \geq \Big(\sum_{k=1}^{n} a_k\Big) \log\Big(\frac{\sum_{k=1}^{n} a_k}{\sum_{k=1}^{n} b_k}\Big) \tag{7}$$

it is easy to see that $I_{r_i}^d \geq 0$ (substituting $a_k$, $b_k$, and $n$ by $\mathcal{F}_{ij}$, $\mathcal{A}_j$, and $n_p$, respectively). From this result, we deduce that $I_r^d \geq 0$.

In [6], we show that for the constant radiosity case the increase in mutual information between two planar patches $i$ and $j$ when subdividing $i$ into $m$ sub-patches is given by

$$(\Delta I_r^d)_{ij} = 2B_i B_j \Big( \big( \sum_{k=1}^{m} A_{i_k} F_{i_k j} \log(F_{i_k j}) \big) - A_i F_{ij} \log(F_{ij}) \Big) \tag{8}$$

From the analysis of this formula, an oracle proposal for hierarchical radiosity refinement was presented. While this oracle was based on the increase of discrete mutual information, the smoothness-based oracle which we will present in the next section is based on the difference between continuous and discrete mutual information.

## 3. Mutual Information Smoothness-Based Oracle

### 3.1. Continuous Radiosity Mutual Information

In [5], we obtained continuous visibility mutual information $I_v^c$ from discrete visibility mutual information $I_v^d$. In a similar way, continuous radiosity mutual information $I_r^c$ can be obtained from $I_r^d$ with the following substitutions:

- $\mathcal{A}_i$ by $\frac{B(x)-E(x)}{\rho(x)} B(x)$
- $\mathcal{A}_T = \sum_i A_i \frac{B_i - E_i}{\rho_i} B_i$ by $\mathcal{A}_T^c = \int_{\mathcal{S}} \frac{B(x)-E(x)}{\rho(x)} B(x) dx$
- $\mathcal{F}_{ij}$ by $\mathcal{F}(x,y) = \frac{\rho(x) F(x,y) B(y)}{B(x) - E(x)}$

where $\mathcal{S}$ represents the surfaces of the scene, $F(x,y)$ is the point-to-point form factor, $B(x)$, $E(x)$, and $\rho(x)$ are respectively the radiosity, self-emitted radiosity, and reflectivity at $x \in \mathcal{S}$.

Thus, we obtain

$$I_r^c = \int_{\mathcal{S}} \int_{\mathcal{S}} \frac{F(x,y) B(x) B(y)}{\mathcal{A}_T^c} \log\Big(\frac{\mathcal{A}_T^c F(x,y)}{B(x)^{in} B(y)^{in}}\Big) dx dy \tag{9}$$

where $B(x)^{in} = \frac{B(x)-E(x)}{\rho(x)}$ represents the incoming radiosity at point $x$. Expression (9) could be computed using the same approach as for the visibility continuous mutual information[5] whenever we know the exact radiosity distribution over the scene and the value of $\mathcal{A}_T^c$. Generally we know neither, so we have to make do with approximate values, computed using a piecewise constant function over all patches. The accuracy of the value found for $I_r^c$ will depend on the quality of this distribution. Applying the following substitutions: $\mathcal{A}_T^c$ by $\mathcal{A}_T$, $B(x)$ by $B_i$, $B(y)$ by $B_j$, $E(x)$ by $E_i$, $E(y)$ by $E_j$, and $R(x)$ by $R_i$, $R(y)$ by $R_j$ , and proceeding as in the visibility case [5], we obtain for $N$ global lines[15]

$$I_r^c \simeq \frac{A_T}{N} \sum_{k=1}^{N} \frac{B_i B_j}{\mathcal{A}_T} \log\Big(\frac{\mathcal{A}_T cos\theta_x cos\theta_y}{\pi d(x,y)^2 B_i^{in} B_j^{in}}\Big) \tag{10}$$

where $B_i^{in} = \frac{B_i - E_i}{\rho_i}$ represents the incoming radiosity on patch $i$, $A_T$ is the total area of the scene, $\theta_x$ and $\theta_y$ are the angles which the normals at $x$ and $y$ form with the line joining them, and $d(x,y)$ is the distance between $x$ and $y$.

### 3.2. Smoothness-Based Oracle

We introduce in this section our information-theoretic oracle based on the radiosity kernel smoothness, to be used in the hierarchical refinement algorithm. As the refinement strategy in hierarchical radiosity deals with a pair of elements at a time, we have to search in our information theory framework for a similar interaction. From the decomposition of expression (9) into a sum over element pairs $\mathcal{S}_i$ and $\mathcal{S}_j$, this

searched for interaction can be expressed by continuous radiosity element-to-element mutual information $I^c_{r_{ij}}$:

$$I^c_{r_{ij}} = \int_{\mathcal{S}_i}\int_{\mathcal{S}_j} \frac{F(x,y)B(x)B(y)}{\mathcal{A}^c_T} \log\Big(\frac{\mathcal{A}^c_T F(x,y)}{B(x)^{in}B(y)^{in}}\Big)\,dxdy \quad (11)$$

This continuous measure expresses with maximum precision the radiosity information transfer between two elements.

The computation of expression (11) will be done with lines joining both elements $i$ and $j$, cast by selecting pairs of random points on both elements (i.e. using $pdf = \frac{1}{A_i A_j}$). Assuming constant approximations for the radiosity over the elements, we obtain for $N_{ij}$ lines:

$$I^c_{r_{ij}} \simeq \frac{A_i A_j B_i B_j}{\mathcal{A}_T} \frac{1}{N_{ij}} \sum_{k=1}^{N_{ij}} F(x_k,y_k) \log\Big(\frac{F(x_k,y_k)\mathcal{A}_T}{B_i^{in}B_j^{in}}\Big) \quad (12)$$

where $x_k$ and $y_k$ are respectively the end-points on path $i$ and $j$ of k-th line. The fundamental idea in our approach is the following: the difference between continuous and discrete element-to-element mutual information gives us a loss of information transfer between two elements due to the discretisation, and at the same time the maximum potential gain of information between them. Thus this difference can be interpreted as a measure for the benefit to be gained by refining and can be used as a decision criterion. Below is an expression showing this difference.

From (4), $I^d_{r_{ij}}$ can be expressed as

$$\begin{aligned} I^d_{r_{ij}} &= \frac{A_i F_{ij} B_i B_j}{\mathcal{A}_T} \log\Big(\frac{F_{ij}\mathcal{A}_T}{A_j B_i^{in} B_j^{in}}\Big) \\ &= \frac{A_i A_j B_i B_j}{\mathcal{A}_T} \frac{F_{ij}}{A_j} \log\Big(\frac{F_{ij}}{A_j}\frac{\mathcal{A}_T}{B_i^{in}B_j^{in}}\Big) \end{aligned} \quad (13)$$

Therefore, taking $\frac{F_{ij}}{A_j} \simeq \frac{1}{N_{ij}}\sum_{k=1}^{N_{ij}} F(x_k,y_k)$, we obtain

$$\begin{aligned} & I^c_{r_{ij}} - I^d_{r_{ij}} \\ \simeq & \frac{A_i A_j B_i B_j}{\mathcal{A}_T}\Bigg(\frac{1}{N_{ij}}\Big(\sum_{k=1}^{N_{ij}} F(x_k,y_k)\log\Big(F(x_k,y_k)\frac{\mathcal{A}_T}{B_i^{in}B_j^{in}}\Big)\Big) \\ & - \frac{F_{ij}}{A_j}\log\Big(\frac{F_{ij}}{A_j}\frac{\mathcal{A}_T}{B_i^{in}B_j^{in}}\Big)\Bigg) \\ = & \frac{A_i A_j B_i B_j}{\mathcal{A}_T}\Bigg(\frac{1}{N_{ij}}\Big(\sum_{k=1}^{N_{ij}} F(x_k,y_k)\log(F(x_k,y_k))\Big) \\ & - \frac{F_{ij}}{A_j}\log\Big(\frac{F_{ij}}{A_j}\Big)\Bigg) \\ = & \frac{A_i A_j B_i B_j}{\mathcal{A}_T}\Bigg(\frac{1}{N_{ij}}\Big(\sum_{k=1}^{N_{ij}} F(x_k,y_k)\log(F(x_k,y_k))\Big) \\ & - \Big(\frac{1}{N_{ij}}\sum_{k=1}^{N_{ij}} F(x_k,y_k)\Big)\log\Big(\frac{1}{N_{ij}}\sum_{k=1}^{N_{ij}} F(x_k,y_k)\Big)\Bigg) \end{aligned} \quad (14)$$

Using the concavity property (7), it is easy to see that $I^c_{r_{ij}} - I^d_{r_{ij}} \geq 0$. This difference gives us the discretisation error between two elements and it is used as the basis for our mutual information (MI) oracle.

Using the above expression as oracle has some inconveniences. First, the value $\mathcal{A}_T$ should be recomputed after each interaction. Second, at the beginning of the radiosity computation most of the receiver $B_i$ values are null. We deal with both problems by dropping $\mathcal{A}_T$ as it does not change much from interaction to interaction and by substituting $B_i$ by $\rho_i$ value as, for a non-source patch, $B_i$ is proportional to $\rho_i$.

Finally, the expression used in the oracle is given by

$$\begin{aligned} \delta = & A_i \rho_i A_j B_j \Bigg(\frac{1}{N_{ij}}\Big(\sum_{k=1}^{N_{ij}} F(x_k,y_k)\log(F(x_k,y_k))\Big) \\ & - \Big(\frac{1}{N_{ij}}\sum_{k=1}^{N_{ij}} F(x_k,y_k)\Big)\log\Big(\frac{1}{N_{ij}}\sum_{k=1}^{N_{ij}} F(x_k,y_k)\Big)\Bigg) \end{aligned} \quad (15)$$

Observe that the receiver area appears weighting the oracle in expression (15), avoiding a too small receiver subdivision.

## 4. Results

We have implemented the classic smoothness–based oracle 2 and our MI one on top of the hierarchical Monte Carlo radiosity [2] method of RenderPark[9] system (`www.renderpark.be`). It shall be noted that our oracle can be used with any hierarchical radiosity method.

The performance of the MI oracle we use two scenes, the *Cornell box* (figures 1 and 4) and the *cube room* (figures 2, 3 and 5). Six different discretisations have been generated for the *Cornell box*: three coarse (figure 1(I)) and three finer ones (figure 1(II)). These discretisations have been obtained from three meshing strategies based respectively on transported power (formula 1) (figures 1(a.I) and 1(a.II)), classic kernel smoothness (formula 2) (figures 1(b.I) and 1(b.II)), and MI kernel smoothness (formula 15) (figures 1(c.I) and 1(c.II)). In a similar way, we compare our strategy with the classic smoothness-based one with two different views of the *cube room* scene (figures 2 and 3). The classic and MI oracles have been evaluated for each discretisation decision with 10 additional point-to-point form factor computation between a pair of elements (except in figures 4 and 5, where 4 rays are used). The power-based oracle has used cheap point–to–polygon form factor estimates.

In figures 1(I) and 1(II) we see the behaviour of the three oracles for two different levels of discretisation. Only in the finer one the shadow of the small cube gets an accurate representation using the power-based and classic smoothness-based oracle, while in the MI one it has already a good representation in the coarse mesh. The power-based oracle overdiscretises the rear wall and the top of the prism, as expected, while the smooth ones correct this effect. However, the MI oracle supports the pass from a coarse to a finer mesh much better (see again the rear wall).

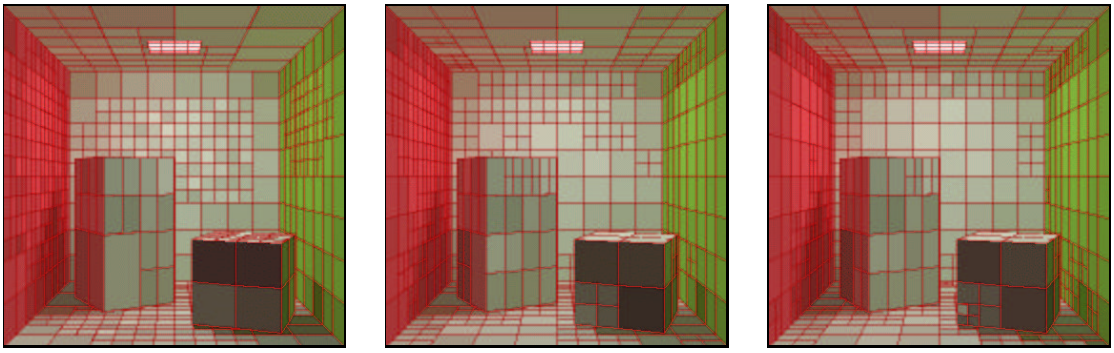

(a.I) Power-based mesh (b.I) Classic smoothness-based mesh (c.I) MI-based mesh

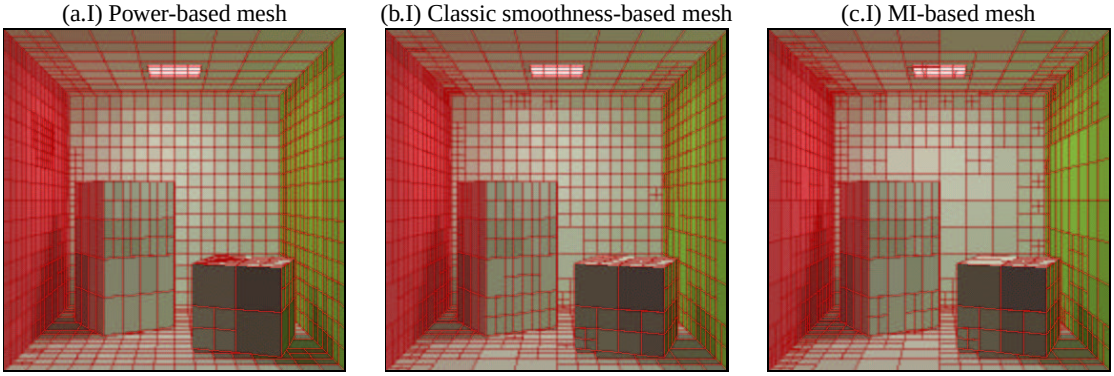

(a.II) Power-based mesh (b.II) Classic smoothness-based mesh (c.II) MI-based mesh

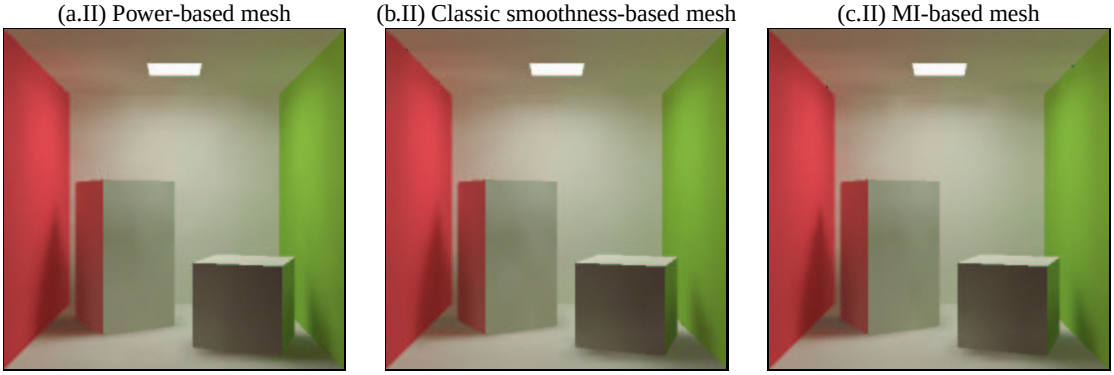

(a.III) Power-based (b.III) Classic smoothness-based (c.III) MI-based

**Figure 1:** *Power-based (a), classic smoothness-based (b) and MI-based (c) methods with the* Cornell box *scene. A coarse mesh is shown in (I) with 1051 (a.I), 1039 (b.I), and 1047 (c.I) patches, with 19472 rays for the radiosity computation. A fine mesh is shown in (II) with 1979 (a.II), 1955 (b.II), and 1995 (c.II) patches, with 116780 rays for the radiosity computation. The Gouraud shaded solution of (II) is shown in (III). For images (b) and (c), 10 rays are cast for each oracle evaluation.*

Figures 2 and 3 show the behaviour of the classic smoothness-based and MI oracle for the *cube room* scene. Observe the accurate representation of the shadow of the chair near the right wall (figure 2(b)) and front wall (figure 3(b)) obtained by the MI oracle. Observe also the much better discrimination in the mesh, seen for instance on the floor and walls, and also the much better represented shadows on the table in figure 3(b).

In figures 4 and 5 the robustness of the classic smoothness-based and MI oracle are tested against a decrease from 10 to 4 point-to-point form factor computation for each oracle evaluation. Classic oracle degenerates to a behaviour similar to the one by power-based oracle, see for instance the rear wall in figure 4(a) (compare with figures 1(b.I)) and the same happens with figure 5(a) (compare with figures 2(a)). On the other hand, the MI oracle keeps most of its good behaviour (compare figure 4(b) with figures 1(c.II)). See also the shadow of the chair near the right wall in figures 5(b) and 2(b).

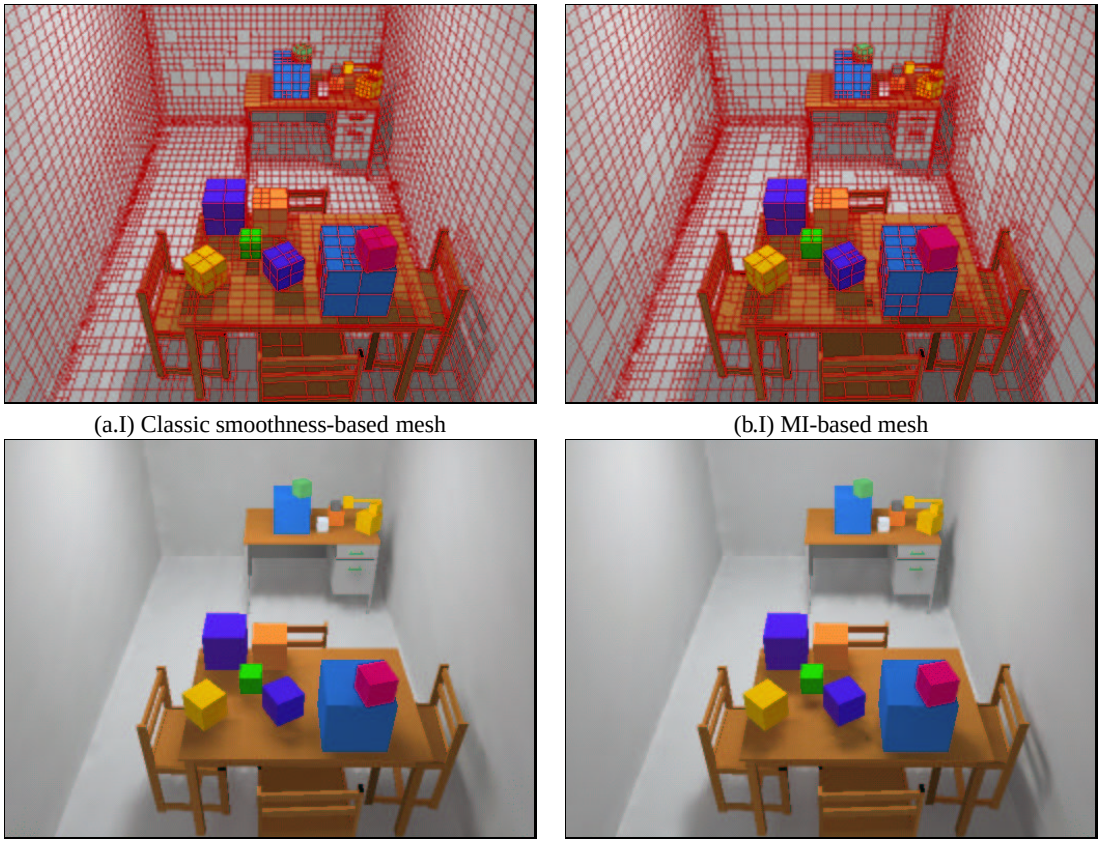

(a.I) Classic smoothness-based mesh (b.I) MI-based mesh

((a.II) Classic smoothness-based (b.II) MI-based

**Figure 2:** *Classic smoothness-based (a) and MI-based (b) methods with the* cube room *scene showing the mesh (I) and Gouraud shaded solution (II). The number of patches is 13902 and 13878 respectively. For each one we cast 402650 rays for radiosity computation and 10 rays for each oracle evaluation.*

## 5. Conclusions

We have introduced in this paper a new smoothness-based refinement oracle for hierarchical radiosity based on the difference between continuous and discrete element-to-element mutual information. This oracle has been compared with the two classic refinement oracles based on transported power and kernel smoothness using a hierarchical Monte Carlo radiosity implementation. Experiments suggest that the newly proposed oracle better preserves illumination detail and avoids overrefinement in smoothly lit areas. It also appears considerably more robust than the classic smoothness-based one.

## Acknowledgements

This project has been funded in part with grant numbers TIC-2001-2416-C03-01 of the Spanish Government and 2001-SGR-00296 of the Catalan Government. All the images have been obtained with the *RenderPark*[9] software. The *Cornell box* reference scene is from Cornell University.

## References

1. Philippe Bekaert. *Hierchical and Stochastic Algorithms for Radiosity*. PhD thesis, Katholieke Universiteit Leuven, Leuven, Belgium, December 1999.

2. Philippe Bekaert, László Neumann, Attila Neumann, Mateu Sbert, and Yves D. Willems. Hierarchical monte carlo radiosity. In George Drettakis and Nelson Max, editors, *Rendering Techniques'98 (Proceedings of the 9th Eurographics Workshop on Rendering)*, pages 259–268, New York (NY), USA, June 1998. Springer-Verlag Vienna-New York. Held in Vienna, Austria.

3. Philippe Bekaert and Yves D. Willems. Error control for radiosity. In Xavier Pueyo and Peter Schöder", editors, *Rendering Techniques'96 (Proceedings of the 7th Eurographics Workshop on Rendering)*, pages 153–164, New York (NY), USA, June 1996. Springer-Verlag Vienna-New York. Held in Vienna, Austria.

4. Thomas M. Cover and Joy A. Thomas. *Elements of*

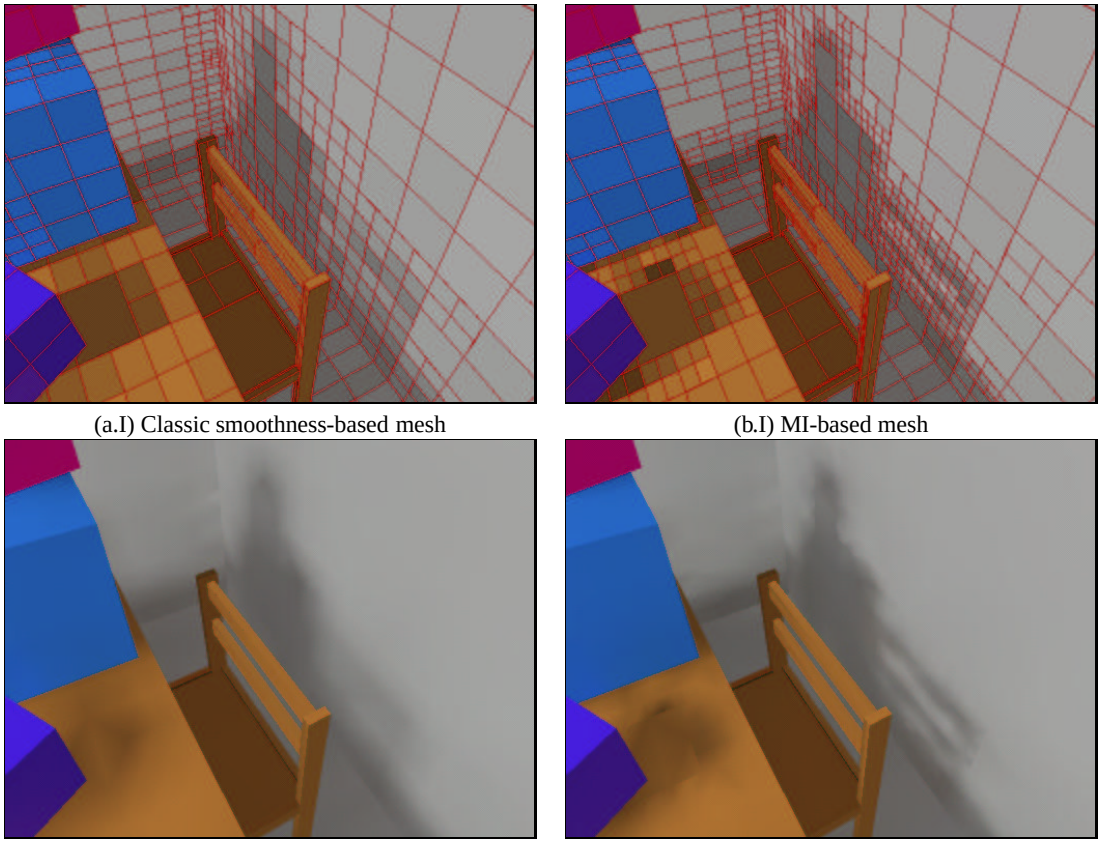

(a.I) Classic smoothness-based mesh (b.I) MI-based mesh

(a.II) Classic smoothness-based (b.II) MI-based

**Figure 3:** *A different view of the scene shown in figure 2.*

*Information Theory*. Wiley Series in Telecommunications, 1991.

5. Miquel Feixas, Esteve del Acebo, Philippe Bekaert, and Mateu Sbert. An information theory framework for the analysis of scene complexity. *Computer Graphics Forum (Proceedings of Eurographics'99)*, 18(3):95–106, September 1999.

6. Miquel Feixas, Esteve del Acebo, Philippe Bekaert, and Mateu Sbert. Information theory tools for scene discretization. In Dani Lischinski and Greg Ward Larson, editors, *Rendering Techniques'99 (Proceedings of the 10th Eurographics Workshop on Rendering)*, pages 95–106, New York (NY), USA, June 1999. Springer-Verlag Vienna-New York. Held in Granada, Spain.

7. Sarah F. Frisken Gibson and Roger J. Hubbold. Efficient hierarchical refinement and clustering for radiosity in complex environments. *Computer Graphics Forum*, 15(5):297–310, 1996.

8. Steven J. Gortler, Peter Schröder, Michael F. Cohen, and Pat Hanrahan. Wavelet radiosity. *Computer Graphics (Proceedings of SIGGRAPH'93)*, 27:221–230, August 1993. Held in Anaheim (CA), USA.

9. Computer Graphics Research Group. *RenderPark: A Photorealistic Rendering Tool*. Katholieke Universiteit Leuven, Leuven, Belgium, November 2000.

10. Pat Hanrahan, David Salzman, and Larry Aupperle. A rapid hierarchical radiosity algorithm. *Computer Graphics (Proceedings of SIGGRAPH'91)*, 25(4):197–206, July 1991. Held in Las Vegas (NV), USA.

11. Nicolas Holzschuch and François Sillion. An exhaustive error-bounding algorithm for hierarchical radiosity. *Computer Graphics Forum*, 17(4):197–218, 1998.

12. Daniel Lischinski, Brian Smits, and Donald P. Greenberg. Bouns and error estimates for radiosity. *Computer Graphics*, 28:67–74, July 1994.

13. Daniel Lischinski, Filippo Tampieri, and Donald P. Greenberg. Combining hierarchical radiosity and discontinuity meshing. *Computer Graphics (Proceedings of SIGGRAPH'93)*, 27:199–208, August 1993. Held in Anaheim (CA), USA.

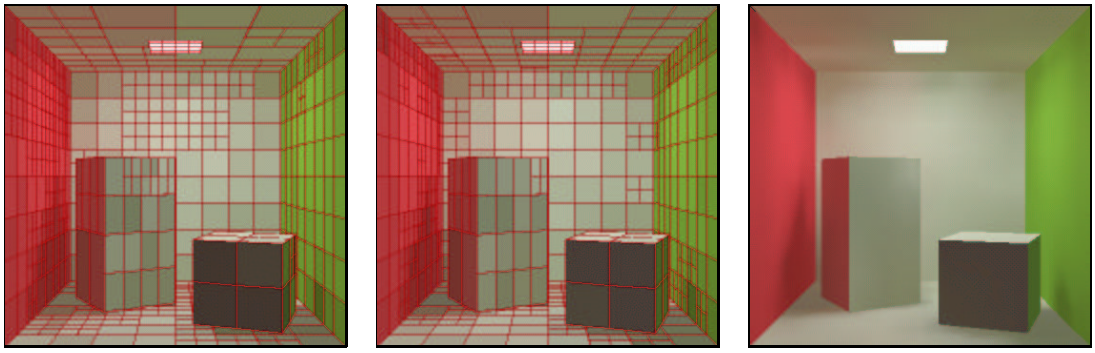

(a) Classic smoothness-based mesh (b) MI-based mesh (c) MI-based

**Figure 4:** *Classic smoothness-based (a) and MI-based (b) methods with the* Cornell box *scene showing the mesh. The number of patches is 875 and 891 respectively. For each one we cast 19458 rays for radiosity computation and 4 rays for each oracle evaluation. The Gouraud shaded solution for (b) is shown in (c).*


14. Sumanta N. Pattanaik and Kadi Bouatouch. Linear radiosity with error estimation. In Pat Hanrahan and Werner Purgathofer, editors, *Rendering Techniques'95 (Proceedings of the 6th Eurographics Workshop on Rendering)*, New York (NY), USA, June 1995. Springer-Verlag Vienna-New York. Held in Dublin, Eire.

15. Mateu Sbert. *The Use of Global Random Directions to Compute Radiosity. Global Monte Carlo Methods*. PhD thesis, Universitat Politècnica de Catalunya, Barcelona, Spain, November 1996.

16. Brian E. Smits, James Arvo, and David Salesin. An importance-driven radiosity algorithm. *Computer Graphics (Proceedings of SIGGRAPH'92)*, 26(2):273–282, July 1992. Held in Chicago (IL), USA.

17. Marc Stamminger, Philipp Slusallek, and Hans-Peter Seidel. Bounded radiosity – illumination on general surfaces and clusters. *Computer Graphics Forum (Proceedings of Eurographics'97)*, 16(3):300–317, 1997.

18. Seth J. Teller and Pat Hanrahan. Global visibility algorithms for illumination computation. *Computer Graphics (Proceedings of SIGGRAPH'93)*, 27:239–246, August 1993. Held in Anaheim (CA), USA.

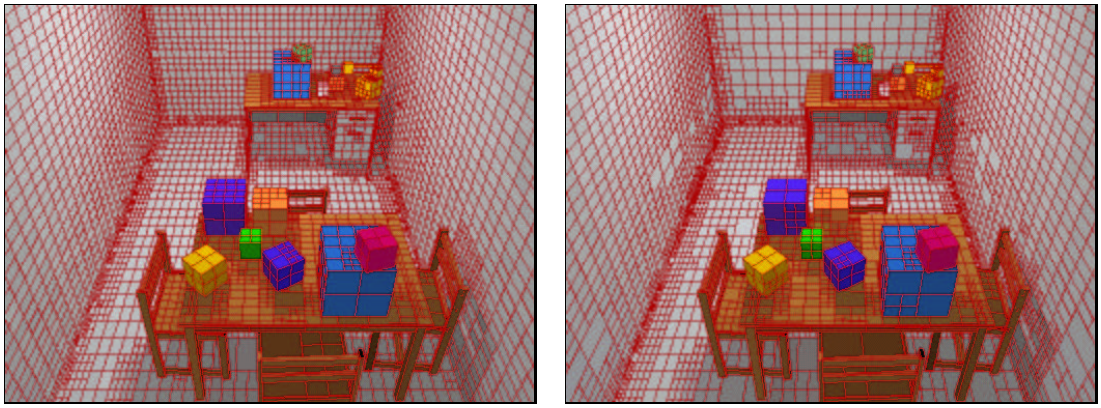

(a.I) Classic smoothness-based mesh (b.I) MI-based mesh

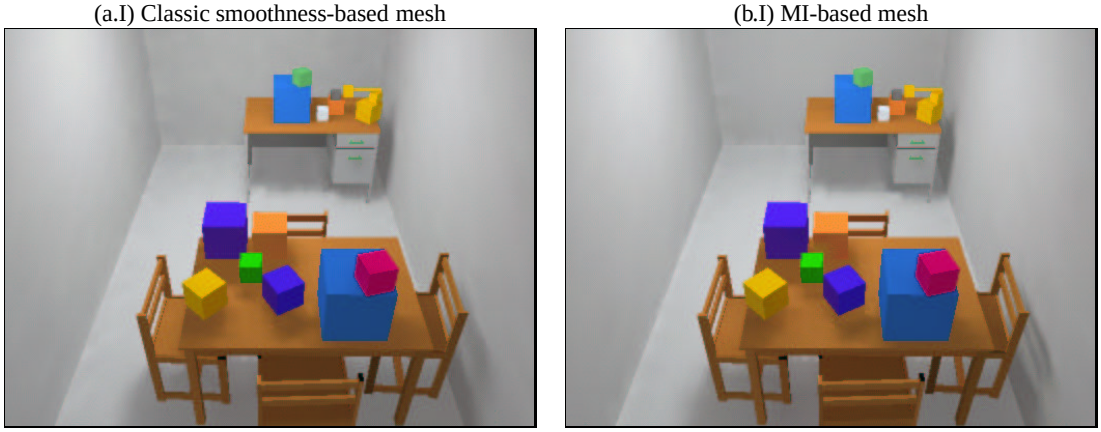

(a.II) Classic smoothness-based (b.II) MI-based

**Figure 5:** *Smoothness-based (a) and MI-based (b) methods with the* cube room *scene showing the mesh (I) and Gouraud shaded solution (II). the number of patches is 13690 and 13758 respectively. For each one we cast 402565 rays for radiosity computation and 4 rays for each oracle evaluation.*